



Universiteit
Leiden
The Netherlands

Liposomal delivery improves the efficacy of prednisolone to attenuate renal inflammation in a mouse model of acute renal allograft rejection

Alem, C.M.A. van; Schmidbauer, M.; Rong, S.; Derlin, K.; Schmitz, J.; Brasen, J.H.; ... ; Rotmans, J.I.

Citation

Alem, C. M. A. van, Schmidbauer, M., Rong, S., Derlin, K., Schmitz, J., Brasen, J. H., ... Rotmans, J. I. (2020). Liposomal delivery improves the efficacy of prednisolone to attenuate renal inflammation in a mouse model of acute renal allograft rejection. *Transplantation*, 104(4), 744-753. doi:10.1097/TP.0000000000003060

Version: Publisher's Version
License: [Creative Commons CC BY-NC-ND 4.0 license](https://creativecommons.org/licenses/by-nc-nd/4.0/)
Downloaded from: <https://hdl.handle.net/1887/3185003>

Note: To cite this publication please use the final published version (if applicable).

OPEN

Liposomal Delivery Improves the Efficacy of Prednisolone to Attenuate Renal Inflammation in a Mouse Model of Acute Renal Allograft Rejection

Carla M.A. van Alem, MSc,¹ Martina Schmidbauer, MD,² Song Rong, PhD,³ Katja Derlin, MD, PhD,² Jessica Schmitz, MSc,⁴ Jan H. Bräsen, MD, PhD,⁴ Anja Thorenz, PhD,³ Rongjun Chen, PhD,³ Jurjen M. Ruben, PhD,¹ Elizabeth M. Winter, MD, PhD,⁵ Maaïke Schilperoort, MSc,⁵ Sander Kooijman, PhD,⁵ Reshma A. Lalai, BSc,¹ Josbert M. Metselaar, PhD,^{6,7} Christian Klemann, MD, PhD,⁸ Martin Meier, PhD,⁹ Cees van Kooten, PhD,¹ Faïkah Gueler, MD, PhD,³ and Joris I. Rotmans, MD, PhD¹

Background. Systemic exposure to high-dose corticosteroids effectively combats acute rejection after kidney transplantation, but at the cost of substantial side effects. In this study, a murine acute renal allograft rejection model was used to investigate whether liposomal-encapsulated prednisolone (LP) facilitates local exposure to enhance its therapeutic effect. **Methods.** Male BalbC recipients received renal allografts from male C57BL/6J donors. Recipients were injected daily with 5 mg/kg cyclosporine A and received either 10 mg/kg prednisolone (P), or LP intravenously on day 0, 3, and 6, or no additional treatment. Functional magnetic resonance imaging (fMRI) was performed on day 6 to study allograft perfusion and organs were retrieved on day 7 for further analysis. **Results.** Staining of polyethylene-glycol-labeled liposomes and high performance liquid chromatography analysis revealed accumulation in the LP treated allograft. LP treatment induced the expression of glucocorticoid responsive gene *Fkbp5* in the allograft. Flow-cytometry of allografts revealed liposome presence in CD45⁺ cells, and reduced numbers of F4/80⁺ macrophages, and CD3⁺ T-lymphocytes upon LP treatment. Banff scoring showed reduced interstitial inflammation and tubulitis and fMRI analysis revealed improved allograft perfusion in LP versus NA mice. **Conclusions.** Liposomal delivery of prednisolone improved renal bio-availability, increased perfusion and reduced cellular infiltrate in the allograft, when compared with conventional prednisolone. Clinical studies should reveal if treatment with LP results in improved efficacy and reduced side effects in patients with renal allograft rejection. (*Transplantation* 2020;104: 744–753)

INTRODUCTION

Acute cellular rejection (ACR) occurs in the early phase after kidney transplantation (KTx) in nearly 10% of all kidney transplant recipients¹ and can complicate the later course of KTx. Acute T-cell-mediated rejection (TCMR)

is characterized in the Banff classifications by significant interstitial inflammation and foci of tubulitis,² and its occurrence can cause decreased long-term graft function.^{3,4}

Received 24 June 2019. Revision received 9 October 2019.

Accepted 20 October 2019.

¹ Department of Internal Medicine, Division of Nephrology, Leiden University Medical Center, Leiden, The Netherlands.

² Institute of Diagnostic and Interventional Radiology, Hannover Medical School, Hannover, Germany.

³ Nephrology, Hannover Medical School, Hannover, Germany.

⁴ Institute of Pathology, Nephropathology Unit, Hannover Medical School, Hannover, Germany.

⁵ Department of Internal Medicine, Division of Endocrinology, Leiden University Medical Center, Leiden, The Netherlands.

⁶ Enceladus Pharmaceuticals, Naarden, the Netherlands.

⁷ Experimental Molecular Imaging, University Clinic, RWTH-Aachen University, Aachen, Germany.

⁸ Department of Pediatric Pneumology, Allergy and Neonatology, Hannover Medical School, Hannover, Germany.

⁹ Institute of Animal Science Imaging Center, Hannover Medical School, Germany. F.G. and J.I.R. contributed equally.

C.M.A.v.A., C.v.K., F.G., and J.I.R. designed the study; C.M.A.v.A., F.G., S.R., R.C., A.T., and M.M. carried out the experiments; C.K. provided all necessary panels, antibodies, machines, and support for FACS; C.M.A.v.A., F.G., R.L., B.M., and M.Schilperoort performed (bio-)medical assays; C.M.A.v.A., C.v.K., F.G., K.D., J.R., E.M.W., M.Schilperoort, S.K., J.S., J.H.B., and M.Schmidbauer analyzed the data; C.v.A., C.v.K., F.G., and J.I.R. drafted and revised the article; all authors read, revised, and approved the final version of the article.

This work was supported by an unrestricted grant from Enceladus Pharmaceuticals, a VIDI grant (016.156.328, J.I.R.), and a research fellowship from the ERA-EDTA Young Fellowship program (RSTF 1223/2017, C.M.A.v.A.).

J.M.M. holds the CEO position at Enceladus Pharmaceuticals.

Supplemental digital content (SDC) is available for this article. Direct URL citations appear in the printed text, and links to the digital files are provided in the HTML text of this article on the journal's Web site (www.transplantjournal.com).

Correspondence: Dr. Joris I. Rotmans, Leiden University Medical Center, Albinusdreef 2, 2333ZA, The Netherlands. (j.i.rotmans@lumc.nl).

Copyright © 2019 The Author(s). Published by Wolters Kluwer Health, Inc. This is an open-access article distributed under the terms of the Creative Commons Attribution-Non Commercial-No Derivatives License 4.0 (CCBY-NC-ND), where it is permissible to download and share the work provided it is properly cited. The work cannot be changed in any way or used commercially without permission from the journal.

ISSN: 0041-1337/20/1044-744

DOI: 10.1097/TP.0000000000003060

High-dose glucocorticoids (GCs) are the cornerstone of TCMR treatment and are deemed successful when a decrease in serum creatinine is observed. Furthermore, GCs are used in low doses as part of the standard triple therapy, frequently combined with a calcineurin inhibitor and mycophenolate mofetil.

The mechanism by which prednisolone exerts its immunosuppressive and anti-inflammatory effects is mediated by genomic- and nongenomic pathways.⁵ Genomic effects are currently explained by free diffusion of prednisolone over the cell membrane and binding to the cytosolic GC receptor (GR) which induces anti-inflammatory effects through transactivation and transrepression of inflammatory factors via nuclear factor kappa-light-chain-enhancer of activated B cells (NF- κ B) and other transcription factors.⁶ The nongenomic effects of GCs are mediated via both classic- and nonclassic GRs associated to the plasma membrane⁷ and are activated at higher doses of GC.⁸ Although GC treatment is frequently effective, systemic administration of GCs results in GR activation in both target and nontarget tissues. Due to this broad bioavailability and high GR affinity, side effects from GC exposure in nontarget tissues can arise both in low and high-dose treatment.⁹ The occurrence of diabetes mellitus, osteoporosis, hypertension, and other side effects related to GC use, pose a significant clinical and economic burden.¹⁰

To prevent nontarget tissue side effects, the systemic availability of prednisolone should be reduced while maximizing target tissue concentrations. Local accumulation in inflamed tissues is therefore highly desirable. A well-studied strategy to achieve this is to encapsulate prednisolone in so-called “long-circulating” poly(ethylene) glycol (PEG)lated liposomes. These liposomes are 100-nm phospholipid bilayer vesicles coated with PEG which allows them to circulate in blood for days upon intravenous (IV) injection. The liposomes prevent the enclosed drug from diffusing over the endothelial lining of blood vessels and subsequently spread over the body, while they are small enough to extravasate and accumulate at inflamed sites where vascular permeability is enhanced.^{11,12} There, macrophages and other phagocytic cells digest the vesicles, releasing the enclosed GC for local action.¹³ One of the advantages of local treatment is the option to reduce the administered total dose, while maintaining an accurate local dose.¹⁴ Previous studies from our group revealed that following IV injection, liposomes accumulate in the inflamed vasculature in a mouse model of arteriovenous fistula failure, and in the inflamed kidney in a rat model of ischemia reperfusion injury.^{15,16} A study in atherosclerotic patients demonstrated local accumulation of liposomal P in plaque macrophages.¹⁷ Despite these encouraging results, there is currently no information on the application of liposomal-encapsulated prednisolone (LP) for TCMR.

In this study, the bio-distribution and efficacy of LP in TCMR was evaluated in a well-characterized model of murine KTx.¹⁸⁻²⁰ LP treatment was compared with conventional P. The main outcome parameters were local accumulation of prednisolone in the allograft and efficacy in reducing allograft rejection.

MATERIALS AND METHODS

Animals

All animal experiments were performed in accordance to Federation for Laboratory Animal Science Associations

guidelines, following approval from the animal protection committee of the Lower Saxony state department for food safety and animal welfare (LAVES), under ethical approval: 14/1569 and 16/2295. Male BALB/c^{HanZtm} (H2^d) mice served as recipients and male C57BL/6J^{HanZtm} (B6; H2^b) mice as donors. All mice were 12–16 weeks old. Animals were housed under normal conditions with free access to standard chow (Altromin 1324) and water. Mice were housed under 14/10 day/night cycle. After surgery, mice were monitored daily for state of health and activity.

Liposomal Formulations

The liposome characteristics have been described previously^{16,21} and a concise summary is included in the **Supplementary Methods** (SDC, <http://links.lww.com/TP/B847>). The liposomes had a mean size of 100 ± 10 nm with a polydispersity index of <0.1 . The zeta potential was consistently -5 mV. In vitro uptake and in vivo distribution characteristics have been described previously, where in vitro uptake by macrophages was initiated within 8 hours and in vivo half-life in rodents was 40 hours.^{15,16,22}

Allogenic KTx Model

The allogenic KTx model was realized by using fully mismatched donors and recipients (B6 H2^b to BALB/c H2^d), which causes acute TCMR within 4–6 days after surgery. The model has been studied extensively and the surgical technique has been described previously.^{18,20,23} Cold and warm ischemia time were standardized (60/30 min) to reduce variability in kidney injury in this model and prevent spontaneous acceptance of the graft.²⁴ A brief protocol is described in **Supplementary Methods** (SDC, <http://links.lww.com/TP/B847>). KTx was performed on day 0, and mice were treated daily with 5 mg/kg cyclosporine A via subcutaneous injections. Cyclosporine A (Novartis, Switzerland) was dissolved in 0.9% saline to 2 mg/mL. On day 0, 3, and 6, they received either Cy5.5-labeled liposomes ($n = 3$), 10 mg/kg P ($n = 10$), or 10 mg/kg LP ($n = 9$), or no additional treatment (NA; $n = 8$) via IV injection. Prednisolone sodium phosphate (Fagron, the Netherlands) was dissolved in 0.9% saline to 4 mg/mL. Mice were sacrificed on day 7 under isoflurane anaesthesia by whole body perfusion with ice-cold phosphate buffered saline. All internal organs, and tibia, quadriceps, femur, and interscapular brown adipose tissue were weighed and processed for further analysis.

MRI

MRI examination was performed as described previously.²⁵ Mice were examined in isoflurane anaesthesia using a 7T small-animal scanner (Bruker, Pharmascan, PHS701, Ettlingen, Germany) with a circularly polarized volume coil (Bruker T10327 V3). A brief description can be found in the **Supplementary Methods** (SDC, <http://links.lww.com/TP/B847>).

Histology and Renal Allograft Morphology

LP was visualized by anti-PEG primary antibody (PEG-B-47b; Abcam, United Kingdom) on 4- μ m frozen sections. Fat area % was determined on hematoxylin and eosin-stained 4- μ m paraffin brown adipose tissue sections. Banff classification was performed by a trained nephropathologist according to the actual consensus on 2 μ m periodic acid Schiff stained

paraffin sections of the allograft.²⁶ Immunohistochemical stainings with CD3 and F4/80 antibodies (SP7 and Cl:A3-1; both from Abcam) were performed on 2 μ m paraffin sections and visualized using Cy3-conjugated secondary antibodies (Jackson ImmunoResearch). Sections were sealed with ProLong Gold Antifade Mountant with 4',6-diamidino-2-phenylindole (Thermo Fisher Scientific). Semiquantitative scoring of the CD3⁺ T-cell and F4/80⁺ macrophage infiltrates was performed at 200-fold magnification on a Leica imaging microscope and scored on a 0–4 scale; 0 = no cells; 1 = <2; 2 = 3–10; 3 = 11–25; 4 = >25 cells and dense cell accumulation.

Flow Cytometry

Kidney tissue was weighed and homogenized by a gentleMACS dissociator (Miltenyi Biotec, Germany) after collagenase II (Worthington Biochemical Corporation) digestion. Seventy micrometer pore filters were used to acquire single cell suspensions and red blood cells were lysed with red blood cell lysis buffer (BioLegend). Cells were counted and stained with live/dead marker (Viability Dye eF506, Thermo Fischer Scientific). Cell surface markers were stained with CD11c-PerCp-Cy5.5 (clone N418) eF506-conjugated Viability Dye, CD3e-PerCp-Cy5.5 (clone 145-2C11) (all from eBioscience Inc.), CD206-FITC (clone MR5D3, Biorad), CD19-PE (clone 1D3, BD), CD45-eF450 (clone 30-F11), F4/80-APC (clone BM8), Ly6C-PE (clone HK1.4), Ly6G-PE-Cy7 (clone 1A8) (all from BioLegend). Samples were spiked with beads to allow for cell counting post-measurement. Uptake of liposomes by infiltrating cells was measured using Cy5.5-labeled liposomes. Flow cytometry was performed on a BD FACSCanto II using FACSDIVA software (both from BD Biosciences). Data were analyzed using FlowJo V10 (FlowJo LLC). Population percentages were translated to cell counts per whole organ, using population percentages, bead density, cell count, and organ weight.

High Performance Liquid Chromatography

Kidney tissue prednisolone content was quantified with high performance liquid chromatography (HPLC) by Ardena Bioanalytical Laboratory (The Netherlands). Briefly, 50 mg of kidney tissue was homogenized, aliquoted, and weighed. Samples were cleaned using methanol and acetonitrile protein precipitation. Following evaporation and reconstitution in acetonitrile/water the samples were analyzed using the API 4000 LC-MS/MS System (Sciex). Quality control samples were spiked at low (0.300 μ g/g), medium (5.00 μ g/g), and high (80.0 μ g/g) levels using prednisolone-D6 standard.

Quantitative Polymerase Chain Reaction

Messenger ribonucleic acid was isolated from frozen tissue or pulverized bones, dissolved in TRIzol (Thermo Fisher Scientific) using a RNeasy mini kit (Qiagen, Germany) according to the manufacturer's protocol. Complementary deoxyribonucleic acid was synthesized using the M-MLV system (Promega) and used for quantitative polymerase chain reaction (qPCR) analysis with SYBR Green master mix (Bio-rad) and gene specific primers (Table S1, SDC, <http://links.lww.com/TP/B847>).

Blood Glucose and Insulin Measurements

Blood glucose levels were determined daily using an Accu-check system (Roche Diabetes Care Inc). At the experimental endpoint, blood was collected from mice

via orbita puncture in ethylenediaminetetraacetic acid tubes and plasma was collected, aliquoted, and stored at -80°C . Plasma insulin was measured using a mouse insulin enzyme-linked immunosorbent assay according to manufacturers' protocol (Mercodia Inc, Sweden).

Liver Cholesterol Measurements

Total liver tissue was homogenized and lipids were extracted using the Folch method. Total cholesterol was determined with a calorimetric assay (11489232; Roche, Switzerland) using Autocal cholesterol standards (6.92 mmol/L; Instruchemie, The Netherlands).

Statistics

Data are presented as mean \pm SD. Statistical analysis was performed using GraphPad Prism 7.00 (GraphPad Software). Comparisons between 2 groups were analyzed using a Student *t*-test, comparisons between allograft and contralateral kidneys with a paired Student *t* test, and comparisons between 3 groups with a 1-way analysis of variance with Tukey correction for multiple testing. *P* < 0.05 was considered statistically significant.

RESULTS

LP Localizes to the Renal Allograft and Accumulates in Macrophages

To analyze the distribution of LP in various organs, kidney transplant recipient mice ($n = 3$) were injected daily with cyclosporine A, and with Cy5.5 loaded liposomes on day 0, 3, and 6, and sacrificed on day 7. Their organs were retrieved and the PEG layer of the liposomes was stained. Liposomes were observed all throughout the allograft in high density (Figure 1B). In the contralateral native kidney of the recipient, liposomes appeared to localize mainly in the glomeruli (Figure 1A). In all 3 mice, mean fluorescence intensity was higher in the allograft than in the contralateral kidney (Figure 1C). In the liver interstitium, stomach, and intestines, liposomes were detected as well, but in much lower density than observed in the allograft. Other organs were devoid of any signal (Figure S1, SDC, <http://links.lww.com/TP/B847>).

The renal allografts of these 3 mice were processed to a single cell suspension and prepared for FACS analysis to determine the distribution of Cy5.5⁺ liposomes in the kidney. To determine which cells had taken up the liposomes, living cells were gated, and subsequently all Cy5.5⁺ cells were selected. This population was composed of mainly CD45⁺ leukocytes (91.5 \pm 3%). Major subpopulations were F4/80⁺ cells and Ly6C⁺ cells (66.4 \pm 1% and 74.0 \pm 2%). Smaller populations were observed in CD206⁺, Ly6G⁺, CD3⁺, and CD19⁺ cells (11.8 \pm 3%, 10.8 \pm 1%, 5.6 \pm 1%, and 3.9 \pm 1%; Figure 2A). Conversely, when looking at the ability of specific cell populations to take up liposomes F4/80⁺ macrophages and CD206⁺ anti-inflammatory macrophages showed 57.5 \pm 12% and 92.3 \pm 4% positivity for the Cy5.5⁺ fluorophore respectively, whereas only 34.5 \pm 12% of CD3⁺ T-cells showed Cy5.5 positivity (Figure 2B).

Altered Bio-distribution Leads to Increased Prednisolone Content in the Inflamed Kidney

KTx recipients were injected with either 10 mg/kg prednisolone ($n = 10$), 10 mg/kg LP ($n = 9$), or received NA ($n = 8$) at day 0, 3, and 6. To determine the local prednisolone

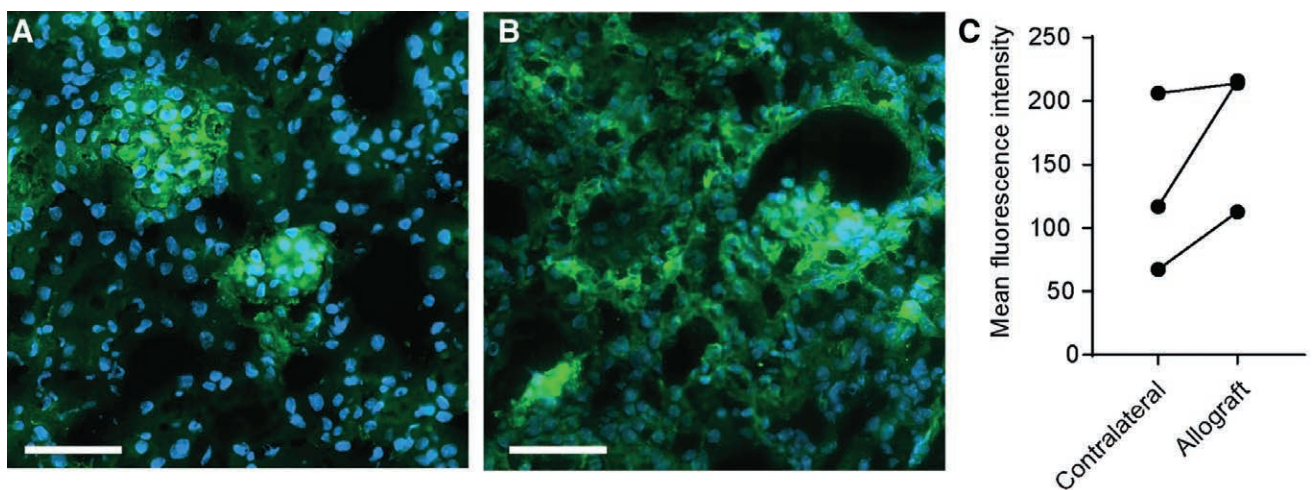


FIGURE 1. Cy5.5⁺ liposome localization in renal allograft recipients. An anti-PEG antibody was used to visualize quenched Cy5.5⁺ liposomes (green), nuclei are visualized by 4',6-diamidino-2-phenylindole (blue). Representative images of (A) the contralateral kidney where liposomes accumulate in the glomeruli, and (B) the allograft where liposomes are present in the glomeruli and throughout the interstitium (scale bar of 50 μ m). C, Quantification of the anti-PEG antibody staining using the mean fluorescence intensity of whole organ sections (MFI). (Data points represent values of individual mice, N = 3 per group). MFI, mean fluorescence intensity; PEG, poly(ethylene) glycol.

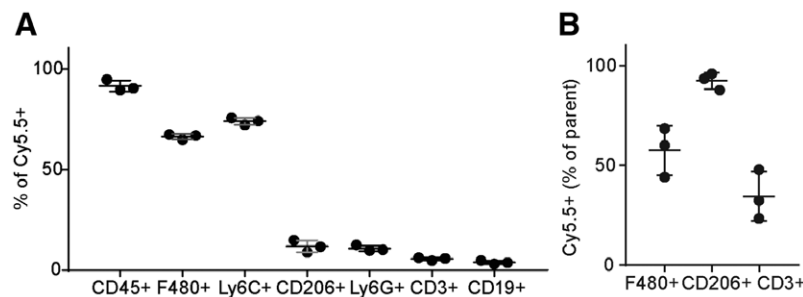


FIGURE 2. The distribution of Cy5.5⁺ liposomes over renal allograft cells. The uptake of Cy5.5⁺ by different cell types in the allograft was analyzed by fluorescence activated cell sorting. A, The living population was gated based on live/dead staining, subsequently, all Cy5.5⁺ cells were gated. Next, gates were placed on leukocyte subpopulations and presented as percentage of parent (Cy5.5⁺). CD45⁺ leukocytes and F4/80⁺ macrophages from the major subgroups. B, From living cells, all F4/80⁺ or CD206⁺ were gated, respectively. Next, a gate was placed on Cy5.5⁺ cells and data were presented as percentage of F4/80⁺ macrophages, CD206⁺ anti-inflammatory macrophages, and CD3⁺ T-cells positive for liposomal signal (Cy5.5). F4/80⁺ macrophages show more internalization of liposomes than CD3⁺ T-cells. (Mean \pm SD, N = 3 per group).

availability in the allograft and the native kidney, HPLC was performed in a subset of mice ($n = 5$ per group). Prednisolone was detected in allografts treated with LP, but not in allografts treated with prednisolone. Tissue from the contralateral kidneys showed some prednisolone presence in LP treated mice but not in prednisolone-treated mice (Figure 3A). Local dose effects of prednisolone were analyzed by monitoring *Fkbp5* mRNA expression, a gene downstream of the GR, which is known to be upregulated up to 24 hours after induction of the receptor.^{27,28} qPCR data showed that LP treatment induced *Fkbp5* to a greater extent than prednisolone and NA treatment in the allograft (3.7-fold and 4.4-fold change, respectively; Figure 3B).

As LP treatment aims to increase local bioavailability and activation of the GR, the occurrence of side effects may be induced locally and were therefore analyzed extensively. The induction of side effects by free prednisolone was measured by analyzing blood glucose and insulin levels by plasma ELISA, determining total liver cholesterol using a calorimetric assay, liver weight, spleen weight, HE staining for brown adipose tissue content, and measuring the degradation of cortical bone by qPCR on bone resorption marker *Trap5b*. Blood glucose levels were unchanged,

and plasma insulin levels also remained stable throughout the follow-up of 7 days in all groups. Brown adipose tissue weight was not affected, nor were liver weight and total liver cholesterol affected when comparing prednisolone or LP to NA treatment. Bone resorption in the tibia was not affected either. However, mice treated with LP did show a reduced spleen weight compared with NA mice (Table S2, SDC, <http://links.lww.com/TP/B847>).

LP Treatment Does Not Affect the Expression of Inflammatory Mediators in the Renal Allograft With TCMR

qPCR were performed to determine the expression of pro- and anti-inflammatory cytokines in the kidney, as readout for the local inflammatory profile. In the NA group, the genes encoding for chemoattractant CCL2 and proinflammatory cytokine TNF α showed an increased expression at day 7 in the allograft compared with the contralateral kidney (Figure 4A). The expression of genes encoding for pro-inflammatory cytokines IL-6 and IL1 β , chemokine CXCL2, and anti-inflammatory cytokine IL-10 did not differ between the allograft and the contralateral kidney after 7 days (Figure 4A). Treatment with either

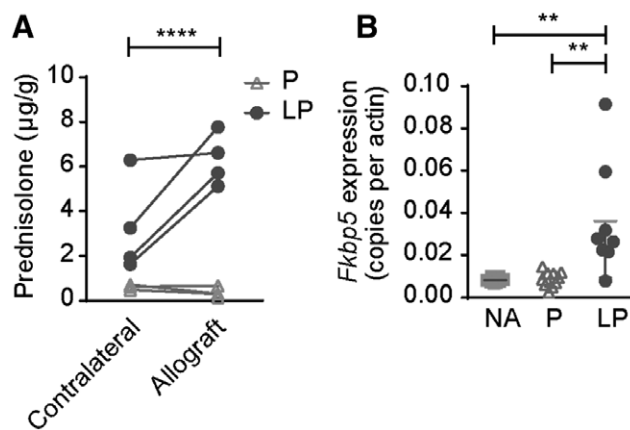


FIGURE 3. Renal prednisolone accumulation after LP treatment. A, Prednisolone concentration in the allograft and contralateral kidney was determined using HPLC. At d 7 post-Tx, prednisolone was detected in higher quantities in allografts of mice treated with LP, but not in allografts of mice treated with P alone. The contralateral native kidney of the recipient treated with LP contained also lower levels of prednisolone. Data points represent individual mice. * $P < 0.05$, unpaired Student's t -test, $N = 4$ per group. B, Messenger RNA expression of the glucocorticoid responsive gene *Fkbp5* in the allografts is plotted as copies per actin. Expression is upregulated in LP-treated allografts, compared with P and NA treated (mean \pm SD. ** $P < 0.01$, one-way analysis of variance with a Tukey multiple comparisons test. NA = no additional treatment; $N = 8$, P = prednisolone; $N = 10$, LP = liposomal prednisolone; $N = 8$. HPLC, high performance liquid chromatography.

prednisolone or LP had no effect on the expression of CCL2 or TNF α compared with NA treatment (Figure 4B). However, when performing qPCR for *Cd45* as a marker for leukocytes, we did observe a significant reduction in the group treated with LP, compared with NA or prednisolone treatment (Figure 4B).

Allograft Cellular Infiltrate Is Reduced Upon Treatment With LP

To determine the effect of LP on infiltrating cells in the allograft, the kidney allografts were digested and dissociated and the composition of this single cell suspension was quantified using FACS analysis. The cell suspension was gated for single cells and subsequently living cells. In line with qPCR data, the amount of CD45⁺ leukocytes was strongly reduced after LP treatment versus prednisolone and NA treatment (372 ± 224 versus 1971 ± 890 and $2440 \pm 948 \times 10^6$ cells, $P < 0.01$ and $P < 0.001$, respectively). When distinguishing different subsets, both a reduction in CD3⁺ T-cells, as well as F4/80⁺ macrophages was observed in the allograft of LP mice (Figure 5).

Allograft rejection was scored using the Banff classification.²⁹ LP treatment reduced interstitial inflammation when compared with prednisolone and NA treatment. Also, tubulitis and peritubular capillaritis were reduced after LP treatment in comparison to NA treatment (Figure 6). In addition, renal interstitial F4/80⁺ macrophages, and CD3⁺ T-cells were detected via immunohistochemistry (Figure 7A). Quantification of these infiltrates revealed a reduced number of CD3⁺ T-cells in the allograft after both prednisolone and LP treatment compared with NA treatment (3.0 ± 0.0 and 2.3 ± 0.0 versus 3.9 ± 0.0 , $P < 0.01$ and $P < 0.001$, respectively), and

F4/80⁺ macrophage infiltrate was also reduced after LP treatment compared with prednisolone or NA (1.9 ± 0.0 versus 3.2 ± 0.0 and 3.8 ± 0.0 , $P < 0.01$ and $P < 0.001$, respectively; Figure 7B). Taken together results of PCR, FACS and immunofluorescence show that LP treatment is more efficient in reducing the TCMR.

Treatment With LP Improved Functional Renal Parameters

In this experimental model, we choose to keep the contralateral kidney in situ to reduce dropout of animals, which precluded the use of serum markers like creatinine or blood urea nitrogen as functional readouts. To determine allograft function, a functional magnetic resonance imaging (fMRI) analysis was performed on day 6 after KT_x, as renal perfusion strongly correlates to the function.^{19,20} Arterial spin labeling allowed for imaging of renal cortex perfusion (Figure 8A). Quantification of these images revealed that renal cortical perfusion was significantly increased in LP treated recipients compared with NA (423.1 ± 100 versus 215.5 ± 107 mL/min \times 100g, $P < 0.05$; Figure 8B).

DISCUSSION

The results obtained in this study show that treatment of acute TCMR of the allograft with LP resulted in a local higher P content compared with conventional treatment with free prednisolone. This altered bio-distribution resulted in a more effective treatment of TCMR, with a greater reduction of cellular infiltrates and a better perfusion of murine renal allografts.

In a previous study in a rat model of ischemia-reperfusion injury, proof of concept was shown in a prednisolone unresponsive model where local accumulation of LP in the inflamed kidney of rats was observed. In that study, liposomes were observed in the interstitial space and glomerular endothelial cells, but not in the podocytes of the glomeruli, indicating that renal uptake was most likely due to enhanced vascular permeability in the inflamed kidney instead of glomerular filtration.¹⁶ This is further substantiated by the size of the particles at 100 nm diameter, while fenestrae in glomerular capillaries do not exceed 15 nm.³⁰ In the present mouse study, this altered bioavailability is confirmed in a model of T-cell-mediated renal allograft rejection. The pattern of bio-availability in other immunologically active organs, as described previously,^{16,22} can be explained by the presence of sinusoidal vasculature with an average fenestrae diameter of 100–200 nm, as present in spleen and liver³⁰ and resident macrophages, which are able to internalize liposomal particles.^{31,32} Differences in particle size can thus affect bio-distribution and should therefore be strictly controlled in clinical application, as is the case in current clinical protocols.²¹ In a previous clinical study with liposomal prednisolone,³³ no signs of liver toxicity were observed.

On a cellular level, liposomes were predominantly present in CD45⁺ cells, and F4/80⁺ macrophages appeared especially efficient in internalizing liposomes. As macrophages are known for their phagocytic capacity and involvement in early stages of an inflammatory cascade, they can be considered the ideal target for LP as influencing macrophage presence can thus affect the downstream inflammatory cascade. In previous studies we have demonstrated rapid in vitro cellular uptake of LP by human macrophages within 8 hours.¹⁶

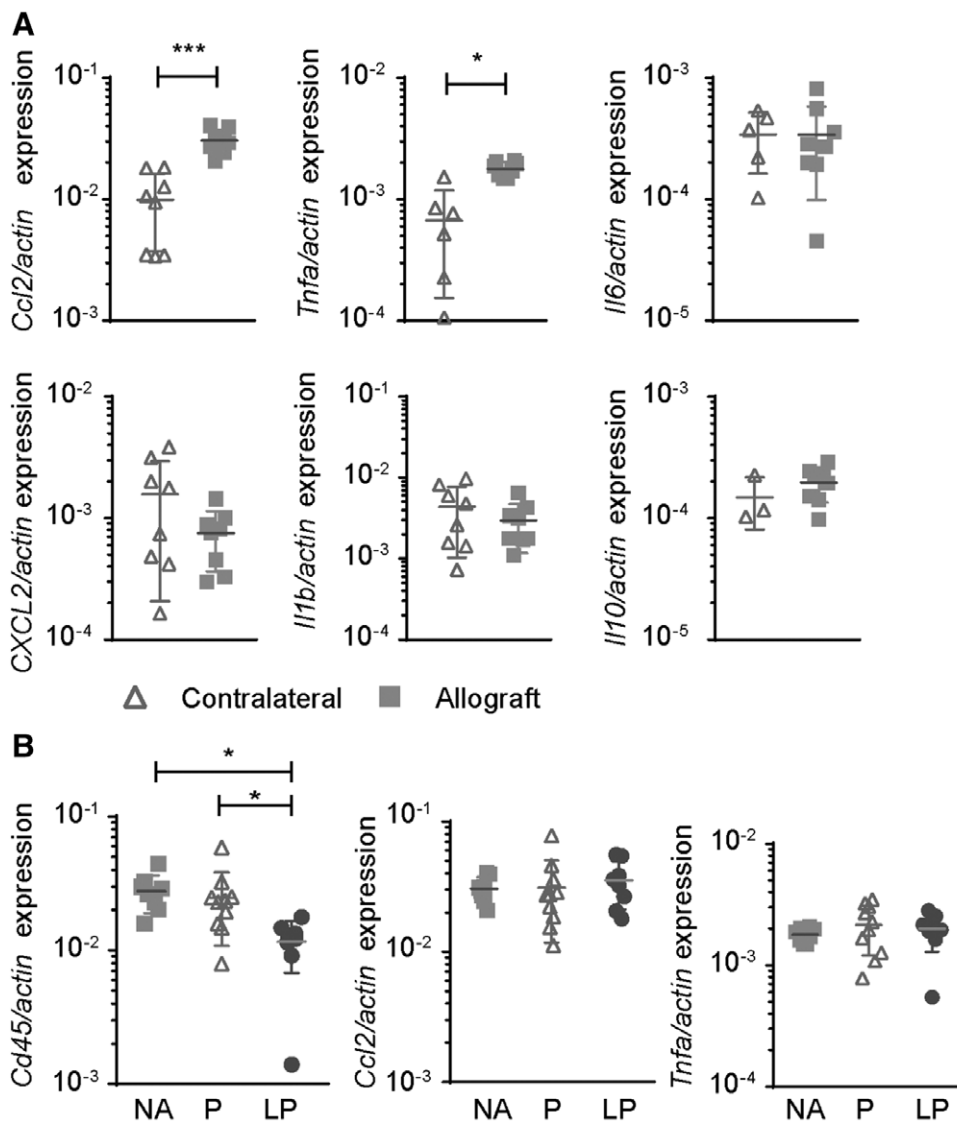


FIGURE 4. CD45 and proinflammatory cytokine expression after LP treatment. A, First, proinflammatory cytokine mRNA expression in allografts vs contralateral kidneys after NA treatment was investigated and showed significant upregulation of Ccl2 and TNF- α , expression in the allografts at d 7. The other investigated cytokines IL-6, CXCL2, IL1- β , and IL10 did not differ compared with the healthy control kidney. B, *Cd45* messenger RNA expression in the allograft was significantly reduced by LP treatment compared with NA or P. Surprisingly, the expression of Ccl2 and TNF-a was similar in the allografts (mean \pm SD. One-way analysis of variance with a Tukey multiple comparisons test. NA = no additional treatment; N = 8, P = prednisolone; N = 10, LP = liposomal prednisolone; N = 8). IL, interleukin; TNF, tumor necrosis factor.

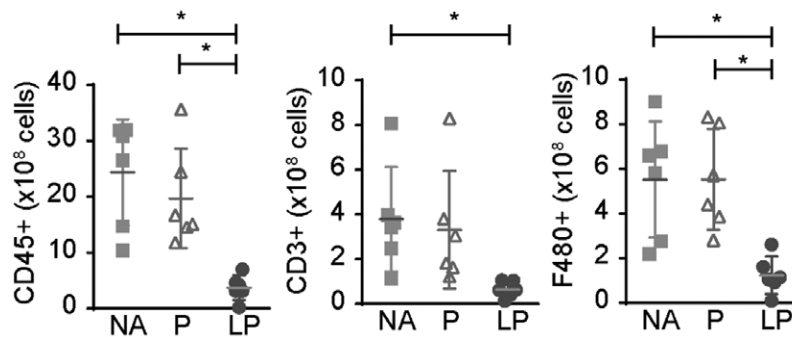


FIGURE 5. The treatment effect of LP on the cellular infiltrate in the allograft. The influx of CD45⁺, CD3⁺, and F4/80⁺ cells after treatment was determined with FACS and calculated to cell count per whole kidney. CD45⁺ and F4/80⁺ infiltrates are reduced after treatment with LP compared with P and NA. CD3⁺ infiltrates are reduced after treatment with LP compared with NA treatment (mean \pm SD. **P* < 0.05, ***P* < 0.01, ****P* < 0.001, one-way analysis of variance with a Tukey multiple comparisons test. NA = no additional treatment; N = 6, P = Prednisolone, N = 6, LP = liposomal prednisolone, N = 6).

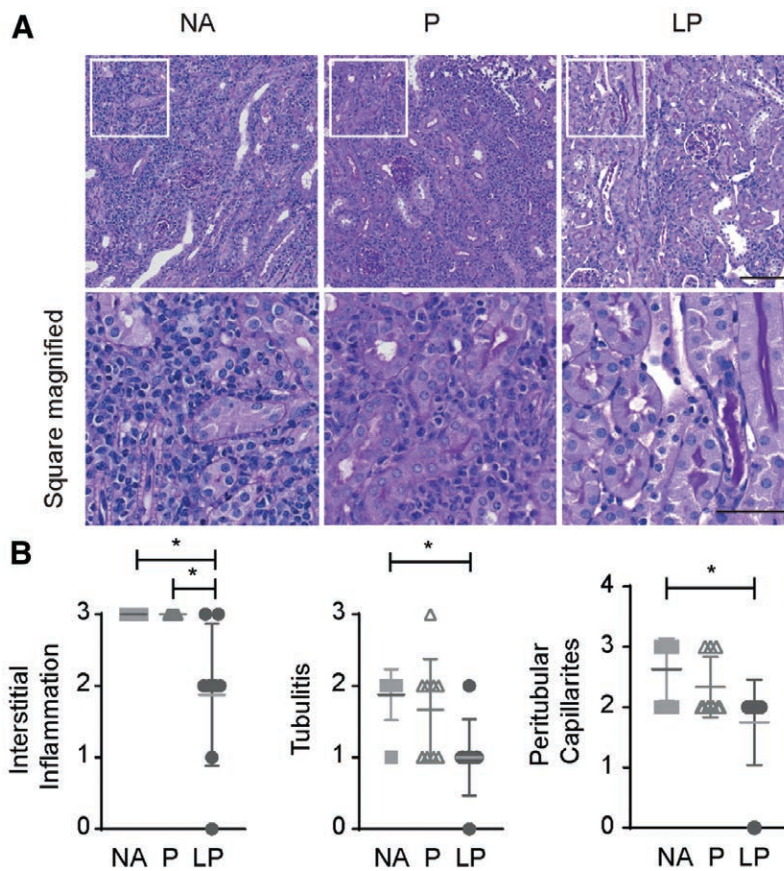


FIGURE 6. Histological evaluation of LP treatment effect. A, PAS stain of allografts showed dense interstitial leukocyte infiltrates in the tubulo interstitial space in the NA and prednisolone-treated groups. However, liposomal prednisolone reduced the inflammation markedly. The upper images are taken at a 200-fold magnification (bar: 100 μ m), the lower images are the enlarged squares of each group to show the differences in infiltrate density (bar: 50 μ m). B, Banff classification of treated allografts reveals decreased interstitial inflammation, tubulitis, and peritubular capillaritis in LP vs NA treatment. Interstitial inflammation is also reduced in LP vs P treatment (mean \pm SD. * $P < 0.05$, 1-way analysis of variance with a Tukey multiple comparisons test. NA = no additional treatment; N = 8, P = prednisolone; N = 9, LP = liposomal prednisolone; N = 9). PAS, periodic acid Schiff.

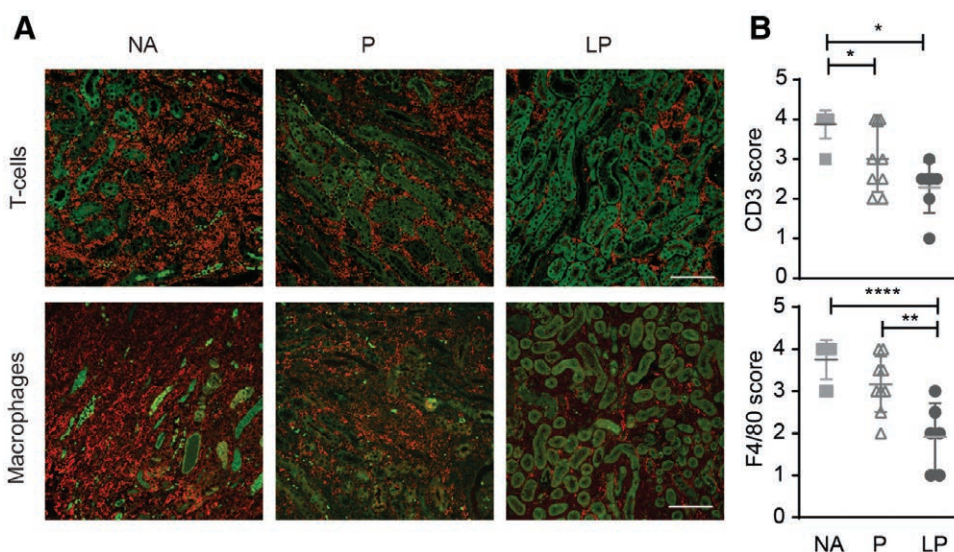


FIGURE 7. LP treatment reduced number of F4/80⁺ macrophages and CD3⁺ T cells in the renal allografts. A, Immunohistochemistry for CD3⁺ T-cells (red, upper panel) and F4/80⁺ macrophages (red) is shown in the allograft. Dense interstitial infiltrates were present in the NA and P group and were markedly reduced in the LP-treated recipients. Green is due to the autofluorescence of the tubuli (bar: 100 μ m). B, Semi-quantitative analysis confirmed that CD3⁺ T-cell infiltration was reduced by prednisolone and even more by LP treatment (NA; N = 8, P; N = 9, LP; N = 7). F4/80⁺ macrophage infiltration was reduced by LP treatment compared with NA or prednisolone (NA; N = 8, prednisolone; N = 9, LP; N = 6) (mean \pm SD. * $P < 0.05$, ** $P < 0.01$, **** $P < 0.0001$, NA = no additional treatment, P = Prednisolone, LP = liposomal prednisolone.

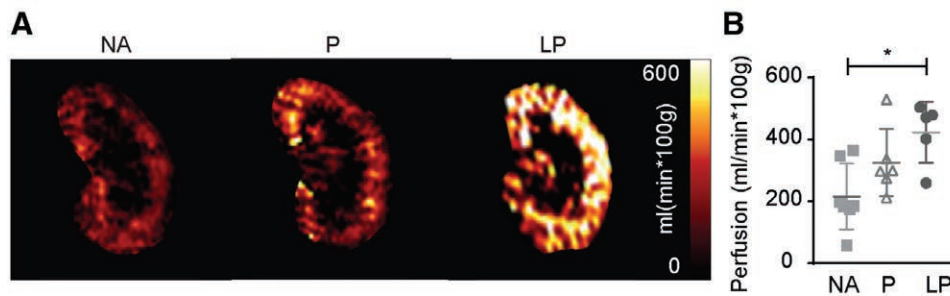


FIGURE 8. Functional evaluation of allograft perfusion by fMRI. A, Representative color-coded perfusion maps of Arterial Spin Labeling (ASL) in functional magnetic resonance imaging shows significantly increased tissue perfusion of the kidney allografts after LP treatment compared with prednisolone and NA treatment. B, The treatment effect of NA, prednisolone, and LP on perfusion is quantified and reveals improved perfusion after LP treatment compared with NA. (Mean \pm SD * P < 0.05, 1-way analysis of variance with a Tukey's multiple comparisons test. N = 7; N = 6, N = 5). LP, liposomal prednisolone; NA, no additional treatment; P, prednisolone.

In the present study, a functional disease model was chosen and HPLC and qPCR analysis revealed increased local concentrations of prednisolone in the allografts after LP versus prednisolone treatment. Achieving locally enhanced tissue concentrations of prednisolone through encapsulation in liposomes for local delivery is a well-studied strategy to reduce systemic exposure and to increase therapy efficacy.^{13,16,32} Although alternative methods to administer immunosuppressive drugs, including local injection, antibody coupling, and protein conjugation, have been described to optimize efficacy and reduce side effects,^{34,35} targeted drug delivery by long-circulating liposomes may be favorable in terms of clinical applicability as extensive clinical experience and a proven safety profile currently favour the use of liposomal drug formulations.³⁶

The current standard treatment of TCMR consists of high doses of IV methylprednisolone which is often effective, although the exact dosing strategy is highly variable among clinical centres.³⁷ Indeed, about 15% of cases are unresponsive to systemic GC infusion and these patients are subsequently treated with anti-thymocyte globulin or monoclonal antibodies.³⁸ The mechanisms underlying GC unresponsiveness are incompletely understood, but recent studies indicate that extensive leukocyte infiltration in the peritubular capillaries and increased expression of cytotoxic T lymphocytes, natural killer cells, B lymphocytes, and macrophages are associated with resistance to GC treatment.³⁹ Also, in patients that do respond to GCs, the efficacy is suboptimal as allograft function frequently does not return to baseline levels. Achieving a higher local dose of prednisolone through liposomal delivery might result in increased drug efficacy as it could target a broader range of infiltrating cells in TCMR.

To assess the efficacy of LP in the treatment of TCMR, the local inflammatory profile, the influx of leukocytes, and the kidney function of the allograft were studied. An increased efficacy of LP was found using histological, FACS, and fMRI analysis, but not at the level of cytokine expression. The cytokine profile in the allograft is determined by cytokine production by inflammatory and epithelial cells.⁴⁰ The lack of a treatment effect on cytokine profile might be attributed to the late time point of the investigation or to the unresponsiveness of renal epithelial cells to GC treatment, which has been demonstrated previously.⁴¹ This lack of association between unchanged cytokine levels and reduced inflammatory cells in the allograft suggests that either direct cell death, or reduced

migration of inflammatory cells upon GC treatment is responsible for its treatment effect.⁴²

Aside from cellular infiltrate composition in the allograft, kidney function is a pivotal factor in evaluating treatment efficacy. Renal function could not be determined by creatinine measurements as 1 native kidney remained in place in this model to avoid unacceptable high mortality upon bilateral nephrectomy in groups with limited treatment efficacy. As previous studies have shown that allograft perfusion closely relates to kidney function,^{19,20} allograft perfusion was evaluated using arterial spin labeling in fMRI. Upon LP treatment, allograft perfusion restored to levels equivalent to isogenic allografts.¹⁹ This suggests a TCMR treatment effect, as other contributing factors, such as acute tubular necrosis, are present throughout all groups and are thought to be unresponsive to prednisolone treatment.

To interpret these findings accurately and translate them to a clinical setting, the limitations of this study need to be considered. To achieve a consistent TCMR model in mice prolonged cold ischemia time of 60 minutes is required. In previous studies several ischemia times were analyzed and revealed spontaneous tolerance of up to 40% in mouse KTx models when ischemia time was kept to <30 minutes. After 60 minutes ischemia time, stable rejection rates within 7 days were achieved. The allograft pathophysiology of this TCMR model was characterized previously in MRI and treatment studies,^{19,20,23,43} allowing for monitoring of LP treatment effects by functional MRI in the present study. Additionally, a triple therapy regime comprising low-dose prednisolone, tacrolimus, and mycophenolic acid could not be administered as such a regime would have prevented the development of TCMR and lead to a model of chronic rejection, precluding the evaluation of LP in the reduction of leukocyte infiltration.⁴⁴ Furthermore, due to the severity of the model, classical long-term side effects of conventional prednisolone therapy could not be determined. In this short-term exposure, no adverse effects from the local dose of LP were observed on plasma glucose or insulin,⁴⁵ brown adipose tissue activation,⁴⁶ liver weight, or total liver cholesterol.⁴⁷ However, a decrease in splenic weight was observed⁴⁸ which might be due to splenocyte depletion or a decrease in edema due to effective suppression of the inflammatory response. In addition, studies utilizing high doses of LP in rats showed limited to no side effects in an extensive analysis, following treatment with LP up to 4 weeks,^{22,32} although it should be noted that GC metabolism in humans is different than in rodents.⁴⁹

Various clinical studies on atherosclerosis, arteriovenous fistula maturation, and ulcerative colitis have evaluated LP safety and efficacy, and extensive experience has been gathered enabling the identification of an optimal dosing regimen for application in humans.^{17,21} This first study in the field of KTx opens up new avenues to explore in clinical care.

In conclusion, this study showed that local accumulation of LP is a promising strategy for targeted treatment of renal allograft rejection and resulted in increased anti-inflammatory efficacy compared to conventional prednisolone. Future clinical studies should reveal if liposomal encapsulation of prednisolone improves its efficacy in TCMR in patients with acute allograft rejection as well.

ACKNOWLEDGMENTS

We thank Ms. H. Chlebush, Ms. T. Streefland, Dr G. Vieten, and Mr C. Bergen for their help with the (bio-) medical assays. Discussions with Prof. P. Rensen and Prof. O. Meijer were also very valuable. The raw data supporting this study are available upon reasonable request.

REFERENCES

- Hart A, Smith JM, Skeans MA, et al. OPTN/SRTR 2015 Annual Data Report: Kidney. *Am J Transplant*. 2017;17(Suppl 1): 21–116.
- Loupy A, Haas M, Solez K, et al. The banff 2015 kidney meeting report: current challenges in rejection classification and prospects for adopting molecular pathology. *Am J Transplant*. 2017;17:28–41.
- Opelz G, Döhler B; Collaborative Transplant Study Report. Influence of time of rejection on long-term graft survival in renal transplantation. *Transplantation*. 2008;85:661–666.
- Naesens M, Kuypers DR, De Vusser K, et al. The histology of kidney transplant failure: a long-term follow-up study. *Transplantation*. 2014;98:427–435.
- Coutinho AE, Chapman KE. The anti-inflammatory and immunosuppressive effects of glucocorticoids, recent developments and mechanistic insights. *Mol Cell Endocrinol*. 2011;335:2–13.
- Barnes PJ, Adcock IM. How do corticosteroids work in asthma? *Ann Intern Med*. 2003;139:359–370.
- Mitre-Aguilar IB, Cabrera-Quintero AJ, Zentella-Dehesa A. Genomic and non-genomic effects of glucocorticoids: implications for breast cancer. *Int J Clin Exp Pathol*. 2015;8:1–10.
- Stellato C. Post-transcriptional and nongenomic effects of glucocorticoids. *Proc Am Thorac Soc*. 2004;1:255–263.
- Stahn C, Buttgerit F. Genomic and nongenomic effects of glucocorticoids. *Nat Clin Pract Rheumatol*. 2008;4:525–533.
- Manson SC, Brown RE, Cerulli A, et al. The cumulative burden of oral corticosteroid side effects and the economic implications of steroid use. *Respir Med*. 2009;103:975–994.
- Sercombe L, Veerati T, Moheimi F, et al. Advances and challenges of liposome assisted drug delivery. *Front Pharmacol*. 2015;6:286.
- Antohe F, Lin L, Kao GY, et al. Transendothelial movement of liposomes in vitro mediated by cancer cells, neutrophils or histamine. *J Liposome Res*. 2004;14:1–25.
- Hofkens W, Storm G, van den Berg WB, et al. Liposomal targeting of glucocorticoids to the inflamed synovium inhibits cartilage matrix destruction during murine antigen-induced arthritis. *Int J Pharm*. 2011;416:486–492.
- Lasic DD. Novel applications of liposomes. *Trends Biotechnol*. 1998;16:307–321.
- Wong C, Bezhaeva T, Rothuizen TC, et al. Liposomal prednisolone inhibits vascular inflammation and enhances venous outward remodeling in a murine arteriovenous fistula model. *Sci Rep*. 2016;6:30439.
- van Alem CMA, Boonstra M, Prins J, et al. Local delivery of liposomal prednisolone leads to an anti-inflammatory profile in renal ischaemia-reperfusion injury in the rat. *Nephrol Dial Transplant*. 2018;33:44–53.
- van der Valk FM, van Wijk DF, Lobatto ME, et al. Prednisolone-containing liposomes accumulate in human atherosclerotic macrophages upon intravenous administration. *Nanomedicine*. 2015;11:1039–1046.
- Rong S, Lewis AG, Kunter U, et al. A knotless technique for kidney transplantation in the mouse. *J Transplant*. 2012;2012:127215.
- Hueper K, Schmidbauer M, Thorenz A, et al. Longitudinal evaluation of perfusion changes in acute and chronic renal allograft rejection using arterial spin labeling in translational mouse models. *J Magn Reson Imaging*. 2017;46:1664–1672.
- Hueper K, Hensen B, Gutberlet M, et al. Kidney transplantation: multiparametric functional magnetic resonance imaging for assessment of renal allograft pathophysiology in mice. *Invest Radiol*. 2016;51:58–65.
- Voorzaat BM, van Schaik J, van der Bogt KE, et al. Improvement of radiocephalic fistula maturation: rationale and design of the liposomal prednisolone to improve hemodialysis fistula maturation (LIPMAT) study - a randomized controlled trial. *J Vasc Access*. 2017;18(Suppl. 1):114–117.
- Lobatto ME, Calcagno C, Otten MJ, et al. Pharmaceutical development and preclinical evaluation of a GMP-grade anti-inflammatory nanotherapy. *Nanomedicine*. 2015;11:1133–1140.
- Gueller F, Shushakova N, Mengel M, et al. A novel therapy to attenuate acute kidney injury and ischemic allograft damage after allogeneic kidney transplantation in mice. *Plos One*. 2015;10:e0115709.
- Zhang Z, Zhu L, Quan D, et al. Pattern of liver, kidney, heart, and intestine allograft rejection in different mouse strain combinations. *Transplantation*. 1996;62:1267–1272.
- Hueper K, Gutberlet M, Rong S, et al. Acute kidney injury: arterial spin labeling to monitor renal perfusion impairment in mice-comparison with histopathologic results and renal function. *Radiology*. 2014;270:117–124.
- Haas M, Loupy A, Lefaucheur C, et al. The banff 2017 kidney meeting report: revised diagnostic criteria for chronic active T cell-mediated rejection, antibody-mediated rejection, and prospects for integrative endpoints for next-generation clinical trials. *Am J Transplant*. 2018;18:293–307.
- Guidotti G, Calabrese F, Anacker C, et al. Glucocorticoid receptor and FKBP5 expression is altered following exposure to chronic stress: modulation by antidepressant treatment. *Neuropsychopharmacology*. 2013;38:616–627.
- Bali U, Phillips T, Hunt H, et al. FKBP5 mRNA expression is a biomarker for GR antagonism. *J Clin Endocrinol Metab*. 2016;101:4305–4312.
- Roufosse C, Simmonds N, Clahsen-van Groningen M, et al. A 2018 reference guide to the banff classification of renal allograft pathology. *Transplantation*. 2018;102:1795–1814.
- Sarin H. Physiologic upper limits of pore size of different blood capillary types and another perspective on the dual pore theory of microvascular permeability. *J Angiogenesis Res*. 2010;2:14.
- Hofkens W, Schelbergen R, Storm G, et al. Liposomal targeting of prednisolone phosphate to synovial lining macrophages during experimental arthritis inhibits M1 activation but does not favor M2 differentiation. *Plos One*. 2013;8:e54016.
- Metselaer JM, Wauben MH, Wagenaar-Hilbers JP, et al. Complete remission of experimental arthritis by joint targeting of glucocorticoids with long-circulating liposomes. *Arthritis Rheum*. 2003;48:2059–2066.
- Barrera P, Mulder S, Smetsers A, et al. Long-circulating liposomal prednisolone versus pulse intramuscular methylprednisolone in patients with active rheumatoid arthritis. Paper presented at: ACR Annual Scientific Meeting 2008; San Francisco, CA.
- Clarke L, Kirwan J. Efficacy, safety and mechanism of action of modified-release prednisone in rheumatoid arthritis. *Ther Adv Musculoskelet Dis*. 2012;4:159–166.
- Look M, Stern E, Wang QA, et al. Nanogel-based delivery of mycophenolic acid ameliorates systemic lupus erythematosus in mice. *J Clin Invest*. 2013;123:1741–1749.
- Aversa F, Busca A, Candoni A, et al. Liposomal amphotericin B (ambisome®) at beginning of its third decade of clinical use. *J Chemother*. 2017;29:131–143.
- Bock HA. Steroid-resistant kidney transplant rejection: diagnosis and treatment. *J Am Soc Nephrol*. 2001;12 (Suppl 17):S48–S52.
- Desvaux D, Schwarzinger M, Pastural M, et al. Molecular diagnosis of renal-allograft rejection: correlation with histopathologic evaluation and antirejection-therapy resistance. *Transplantation*. 2004;78:647–653.
- Rekers NV, de Fijter JW, Claas FH, et al. Mechanisms and risk assessment of steroid resistance in acute kidney transplant rejection. *Transpl Immunol*. 2016;38:3–14.
- Stadnyk AW. Cytokine production by epithelial cells. *Faseb J*. 1994;8:1041–1047.
- de Haij S, Woltman AM, Bakker AC, et al. Production of inflammatory mediators by renal epithelial cells is insensitive to glucocorticoids. *Br J Pharmacol*. 2002;137:197–204.

42. Kim BY, Son Y, Lee J, et al. Dexamethasone inhibits activation of monocytes/macrophages in a milieu rich in 27-oxygenated cholesterol. *Plos One*. 2017;12:e0189643.
43. Hueper K, Gutberlet M, Bräsen JH, et al. Multiparametric functional MRI: non-invasive imaging of inflammation and edema formation after kidney transplantation in mice. *Plos One*. 2016;11:e0162705.
44. Muntean A, Lucan M. Immunosuppression in kidney transplantation. *Clujul Med*. 2013;86:177–180.
45. Pagano G, Cavallo-Perin P, Cassader M, et al. An in vivo and in vitro study of the mechanism of prednisone-induced insulin resistance in healthy subjects. *J Clin Invest*. 1983;72:1814–1820.
46. van den Beukel JC, Grefhorst A, Quarta C, et al. Direct activating effects of adrenocorticotrophic hormone (ACTH) on brown adipose tissue are attenuated by corticosterone. *Faseb J*. 2014;28:4857–4867.
47. Liu YF, Wei JY, Shi MH, et al. Glucocorticoid induces hepatic steatosis by inhibiting activating transcription factor 3 (ATF3)/S100A9 protein signaling in granulocytic myeloid-derived suppressor cells. *J Biol Chem*. 2016;291:21771–21785.
48. Voetberg BJ, Garvy BA, Mayer HK, et al. Apoptosis accompanies a change in the phenotypic distribution and functional capacity of murine bone marrow B-cells chronically exposed to prednisolone. *Clin Immunol Immunopathol*. 1994;71:190–198.
49. Rose JQ, Yurchak AM, Jusko WJ. Dose dependent pharmacokinetics of prednisone and prednisolone in man. *J Pharmacokinet Biopharm*. 1981;9:389–417.